



Effects of exact kinematics and the Sudakov form factor on the dipole amplitude

T. Goda, K. Kutak^a, S. Sapeta

The H. Niewodniczański Institute of Nuclear Physics PAN, Radzikowskiego 152, 31-342 Kraków, Poland

Received: 29 May 2023 / Accepted: 24 September 2023 / Published online: 24 October 2023
© The Author(s) 2023

Abstract We investigate the effects of exact gluon kinematics on the parameters of the Golec-Biernat–Wüsthoff, and Bartels–Golec-Biernat–Kowalski saturation models. The resulting fits show some differences, particularly, in the normalization of the dipole cross section σ_0 . The refitted models are used for the dijet production process in DIS to describe HERA data and investigate the effects of the Sudakov form factor at the future Electron Ion Collider.

1 Introduction

Factorization of scales plays central role in *Quantum Chromodynamics* (QCD). In particular, within collinear factorization approach, long-distance effects can be isolated into objects called *collinear parton distribution functions* (PDFs) [1, 2]. The collinear PDFs are not fully perturbatively calculable but they obey perturbative evolution equations and are process-independent [2]. That is to say that one needs to determine initial condition by fit to data, and the obtained PDFs can be used universally.

One of the main type of processes that is suited particularly well to the studies of proton structure is the *deep inelastic scattering* (DIS) [1, 2]. The data from HERA has enabled us to answer many questions in that domain and largely improved our picture of interior of a proton. It is therefore very exciting that the next generation of DIS machines, the Electron Ion Collider (EIC) [3] is making its way and will soon allow us to uncover more details about hadron structure.

At large center of mass energy and fixed value of the photon virtuality, Q , one probes the region of small Bjorken scaling variable, x . In that region, which is dominated by gluons [1, 2, 16], the approach of High Energy Factorization, also called k_T -factorization [4–9], has proven to be suited particularly well. In this framework, the interaction of the

photon with gluons happens through boson-gluon fusion or quark impact factor, as depicted in Fig. 1. An object, which is central to the description of such process is called the dipole gluon density, $\mathcal{F}^{\text{dipole}}(x, k_T^2)$, and it is a type of *transverse momentum dependent* (TMD) [10–13] PDF. Due to its clear picture, one often uses a position-space counterpart of the gluon density, called *dipole cross section*. It appears in the k_T -factorization formula [5, 11–13], which we shall discuss in the next section, and plays a role similar to that of the collinear parton distribution function in the collinear factorization.

Much effort has been made to study this object, notably the work of Balitsky, Fadin, Kuraev and Lipatov (BFKL) [14, 15] has predicted sharp rise of cross sections with $1/x$. However, such rise violates unitarity and the Froissart bound [1, 2, 16, 17]. In Ref. [18] it has been recognized that gluon recombination can tame the growth of gluons. The interplay of linear and nonlinear terms leads to a phenomenon called *gluon saturation* and corresponding evolution equations are known as Balitsky–Kovchegov (BK) [19, 20] equation or JIMWLK [21–26] equation.

Despite the success of the aforementioned evolution equations, there exist a number of phenomenological models of the dipole cross section, which are popular due to their simplicity. A notable example is the model proposed by Golec-Biernat and Wüsthoff (GBW) [27] and its extension by Bartels, Golec-Biernat and Kowalski (BGK) [28]. We will use these two specific models in our study. We note, however, that other saturation models have been discussed in the literature [29–32].

In the present study, we fit the GBW and BGK models to HERA data [33] in the k_T -factorization formula for F_2 , instead of the original dipole factorization [34] formula. As discussed below, this allows us to relatively easy investigate the role of the exact gluon kinematics. Since inclusive observables do not reveal the k_T dependence well, in order

^ae-mail: krzysztof.kutak@ifj.edu.pl (corresponding author)

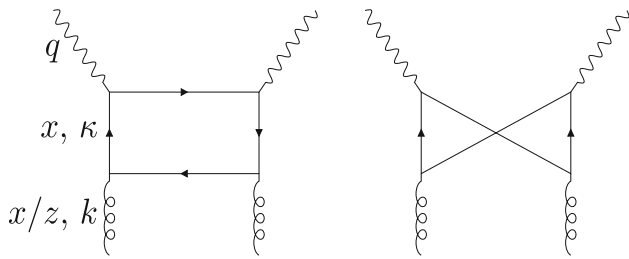


Fig. 1 Kinematic variables of the inclusive DIS

to demonstrate the effects of exact kinematics we consider a less inclusive observable which is more sensitive to the k_T dependence of the gluon distribution. The resulting models are used for predictions of dijet production in DIS at Electron Ion Collider (EIC) [35], including effects of the Sudakov form factor, which resums logarithms of the small transverse momentum. This process is known to be sensitive to another type of gluon density, called Weizsäcker–Williams (WW) [11, 12]. For that process, we study, in particular, the angular correlation of jets, and that of the scattered electron and the jets. For other papers addressing dijet production at the EIC we refer the Reader to [36–40].

The paper is organized as follows. In the next section, we present theoretical framework which we use and outline differences between the k_T -factorization and the dipole factorization. In Sect. 3, results of the new fits to HERA data in the k_T -factorization formula are presented. In Sect. 4, we apply the results from the previous section to compute distributions for dijet production in DIS at the EIC and make comparisons to our earlier study of Ref. [41].

2 The framework

The DIS cross section (structure function) factorises and can be written in a form

$$d\sigma = \sum_a \phi_{a/h} \otimes H_{\gamma a \rightarrow X}, \tag{1}$$

where the hard function, $H_{\gamma a \rightarrow X}$, involving a parton a in the initial state, is calculable perturbatively, and $\phi_{a/h}$ is the parton distribution function of a in a hadron h . The symbol \otimes denotes appropriate convolution. All non-perturbative effects are absorbed in $\phi_{a/h}$, while $H_{\gamma a \rightarrow X}$ can be computed order by order in α_s .

We will study factorization in two versions: defined in momentum and position space, respectively. As mentioned earlier, in the fit, we use the GBW and BGK models. The models were originally formulated in the position-space ver-

sion of the k_T -factorization formula. In the GBW model, the dipole cross section has the form [27]

$$\sigma_{\text{GBW}}(x, r) = \sigma_0 \left(1 - e^{-r^2/R_0^2}\right) \quad \text{where } R_0^{-2} = \frac{Q_0^2}{4} \left(\frac{x_0}{x}\right)^\lambda. \tag{2}$$

The dipole cross section is related to the dipole gluon density by the Fourier transform

$$\alpha_s \mathcal{F}^{\text{dipole}}(x, k_T^2) = \frac{N_c}{4\pi} \int \frac{d^2\mathbf{r}}{(2\pi)^2} e^{i\mathbf{k}_T \cdot \mathbf{r}} \nabla_{\mathbf{r}}^2 \sigma_{\text{dipole}}(x, r). \tag{3}$$

The essence of the GBW model is encoded in the x -dependent saturation scale $Q_s^2(x) = Q_0^2(x_0/x)^{-\lambda}$, which separates the saturation region and the scaling region. An extension of the above model was proposed by Bartels et al. [28] who incorporated the DGLAP evolution in the GBW dipole cross section (2) by modifying the exponent to

$$R_0^{-2} = \frac{\pi^2 \alpha(\mu^2) x g(x, \mu^2)}{3\sigma_0}, \tag{4}$$

where

$$\mu^2 = \frac{C}{r^2} + \mu_0^2 \quad \text{and} \quad x g(x, Q_0^2) = A_g x^{-\lambda_g} (1-x)^{5.6}, \tag{5}$$

thus improving the description of data at higher Q^2 .

While these models enjoyed much success in the phenomenology of DIS, including the diffractive and photo-production processes [27, 42], it is worth mentioning that they both use certain kinematic approximation which is specific to LO dipole factorization and are not there in the k_T -factorization. This was recognized in [43]. In the following, we will investigate effects of these approximations.

Firstly, let us outline the factorization formulas. With $q' \equiv q + xp$, one decomposes k and κ , defined in Fig. 1, as

$$\kappa = \alpha p - \beta q' + \kappa_T \quad \text{and} \quad k = \alpha p - b q' + k_T. \tag{6}$$

For the contribution depicted in Fig. 1, the structure function F_2 factorizes with a change of variable $\kappa'_T \equiv \kappa_T - (1-\beta)\mathbf{k}_T$, to the form [44, 45]

$$F_2(x, Q^2) = \sum_f e_f^2 \frac{Q^2}{2\pi} \int \frac{dk_T^2}{k_T^2} \int_0^1 d\beta \int d\kappa'_T \alpha_s(\mu^2) \times \mathcal{F}^{\text{dipole}}(x/z, k_T^2) \Theta(1-x/z) \times \left[(\beta^2 + (1-\beta)^2) \left(\frac{I_1}{2\pi} - \frac{I_2}{2\pi} \right) + (m_f^2 + 4Q^2\beta^2(1-\beta)^2) \left(\frac{I_3}{2\pi} - \frac{I_4}{2\pi} \right) \right], \tag{7}$$

where

$$\frac{1}{z} = 1 + \frac{\kappa'^2_T + m_f^2}{\beta(1 - \beta)Q^2} + \frac{k_T^2}{Q^2}. \tag{8}$$

One should note that the gluons are not probed directly, thus the argument of the gluon density is x/z rather than x . If one, instead, uses $1/z = 1 + 4m_f^2/Q^2$ and assumes that μ is independent of κ' and k_T , the above formula can be written in the impact parameter space [27,46] (i.e. as a dipole factorization formula)

$$F_2(x, Q^2) = \sum_f e_f^2 \frac{Q^2}{4\pi^2} \int_0^1 d\beta \int \frac{d^2\mathbf{r}}{(2\pi)^2} \times |\Psi(\tilde{x}, \beta, Q^2)|^2 \sigma_{\text{dipole}}(\tilde{x}, r), \tag{9}$$

where the photon wave function, $|\Psi(\tilde{x}, \beta, Q^2)|^2$, describes splitting of the incoming photon into a $q\bar{q}$ pair with light-cone momenta fractions β and $1 - \beta$ respectively, and the dipole cross section, $\sigma_{\text{dipole}}(\tilde{x}, r)$, describes the interaction of the colour dipole of size r with the proton. In Ref. [27], $\tilde{x} = x(1 + 4m_f/Q^2)$ with nonzero value of m_f was used even for light flavours, which is necessary to partially substitute k_T and κ'_T in Eq. (8). In the present study, we use Eq. (7) to fit the models, where the gluon density is obtained by evaluating Eq. (3).

Considering the small- r limit of the GBW model

$$\sigma_{\text{GBW}}(x, r)|_{r \ll Q_s} \approx r^2 Q_s^2/4, \tag{10}$$

comparison to

$$\sigma_{\text{BGK}}(x, r)|_{r \ll Q_s} \approx \frac{r^2 \pi^2 \alpha_s(\mu^2) x g(x, \mu^2)}{3}, \tag{11}$$

from BGK, suggests that the GBW model is an approximation in which $\alpha_s(\mu^2)$ and $xg(x, \mu^2)$ are independent of r [28]. For this reason, in one version of the model discussed below, we shall account for the running coupling in Eq. (7) by assuming that α_s in Eq. (3) is constant for the GBW model, and thus explicitly multiply it by the running coupling

$$\alpha_s(\mu^2) \mathcal{F}^{\text{dipole}}(x, k_T^2) \rightarrow \alpha_s(\mu) \frac{\alpha_s \mathcal{F}^{\text{dipole}}(x, k_T^2)}{0.2}, \tag{12}$$

where

$$\alpha_s(\mu^2) = \frac{1}{\frac{11C_A - 2n_f}{12\pi} \log\left(\frac{\mu^2}{\Lambda_{\text{QCD}}^2}\right)}, \tag{13}$$

and $\Lambda_{\text{QCD}}^2 = 0.09 \text{ GeV}^2$.

The factor 0.2 is an arbitrary normalization, whose effect is absorbed by σ_0 , and hence bears no importance. (For a more detailed analysis of the dipole gluon density from the

BGK model see Ref. [47]¹) While there is some ambiguity on what the argument of $\alpha_s(\mu^2)$ should be, we follow Ref. [45] and use

$$\mu^2 = k_T^2 + \kappa'^2_T + m_f^2 + \mu_0^2, \tag{14}$$

where we add $\mu_0^2 = 4 \text{ GeV}^2$ in order to freeze the coupling at low scales.

3 Fits to F_2 data

We fitted the GBW and BGK models to the F_2 data from HERA [33].² A numerical program was written with help of CERNLIB (DPSIPG) [49], GSL [50], CUBA [51] and ROOT [52] libraries to evaluate F_2 . The fitting was performed using MnMigrad and MnSimplex of ROOT::Minuit2 [53].

The data were selected to be in the range $0.045 \leq Q^2 \leq 650 \text{ GeV}^2$, $x < 0.01$. As with the previous fit [54], the c and b flavours were taken into account with the mass 1.3 and 4.6 GeV, respectively. As discussed earlier, we take the light quarks to be massless.

We studied the following cases

- GBW model with the fixed coupling in k_T -factorization (k_T -GBW),
- GBW model with the running coupling in k_T -factorization (rc- k_T -GBW),
- BGK model in k_T -factorization (k_T -BGK),

and, as a reference, we provide the following results from Ref. [54]

- GBW model with massless light quarks in the dipole factorization (r -GBW),
- GBW model with massive light quarks in the dipole factorization (r -GBW-massive),
- BGK model in the dipole factorization (r -BGK).

The results of the fits are summarized in Table 1. The fit quality of k_T -GBW is almost unchanged w.r.t. r -GBW, while rc- k_T -GBW shows remarkable improvement, almost halving the χ^2 value. This is in line with the observation made in Refs. [55–57] that in the BK evolution, the running coupling corrections have considerable effect.

¹ In Ref. [47], the coupling constant was treated differently and the large k_T -region was matched to the derivative of $xg(x)$, while we have used series transformation to accelerate the high- k_T integration. Their treatment is also different from the original BGK paper [28]. As a consequence, their gluon density is positive in the large k_T -region and the overall large- k_T behaviour is significantly different.

² For description of F_2 at NLO accuracy within dipole factorisation see Ref. [48].

Table 1 Fit parameters of respective models. The parameters of the dipole factorization cases are from Ref. [54]

–	σ_0 [mb]	x_0 (10^{-4})	λ	χ^2/dof		
<i>r</i> -GBW	1.907e+01	2.582e+00	3.219e−01	4.438e+00		
<i>r</i> -GBW-massive	2.384e+01	1.117e+00	3.082e−01	5.274e+00		
k_T -GBW	3.344e+01	1.333e+00	3.258e−01	4.396e+00		
rc- k_T -GBW	1.520e+01	2.648e+00	3.211e−01	2.447e+00		
–	σ_0 [mb]	A_g	λ_g	C	μ_0^2 [GeV ²]	χ^2/dof
<i>r</i> -BGK	2.326e+01	1.181e+00	8.317e−02	3.294e−01	1.873e+00	1.556e+00
k_T -BGK	3.470e+01	1.048e+00	2.205e−01	2.391e−01	9.954e−01	1.527e+00

Another notable point is that, except for the normalization σ_0 , the parameters are very similar, particularly those of rc- k_T -GBW are almost identical to those of *r*-GBW. While the GBW model remains almost unaffected, the BGK model seems to show slightly more change. The difference in σ_0 is similar to that of GBW and other parameters changed moderately.

In Fig. 2, the plots of the dipole cross section, the dipole gluon density and the saturation scale for the GBW and BGK models are shown. The dipole cross section and the gluon density are both normalized by σ_0 in order to show the effects of other parameters better, and the saturation scale is defined as a ridge of the dipole gluon density in the (x, k_T^2) plane.

In the plots on the left hand side, one can see the effects of changes in the parameters of the GBW model. The difference between the rc- k_T -GBW and *r*-GBW is negligible, while the k_T -GBW is slightly shifted, compared to others, by the change in x_0 .

On the right hand side of Fig. 2, the same plots are shown for the BGK model. Unlike in the GBW case, the connection between the differences shown in the plots and the differences in the parameters is less clear. Nevertheless, the differences are more prominent in the small- x region.

Comparisons of the results with the F_2 data are shown in Figs. 3 and 4. In Fig. 3, the differences between *r*-GBW and k_T -GBW are not visible, while rc- k_T -GBW shows sizeable difference from the others, particularly in the large- Q^2 region. Recalling that the parameters of rc- k_T -GBW and *r*-GBW are very similar, the difference in F_2 is almost entirely due to the coupling constant. The improvement in the fit quality is depicted as a histogram of the χ^2 -value per number of points at the bottom of Fig. 3. Here, the improvement in the large- Q^2 region is very clear. In Fig. 4, the differences between *r*-BGK and k_T -BGK are hardly visible. In the histogram at the bottom, one can see some differences, but they cancel out mostly, making little improvement overall.

Let us now take a closer look at the parameter σ_0 . Recall that the difference between the k_T -factorization formula and the dipole factorization formula is in x/z , and this enters in

the GBW formalism as \tilde{x} . It is easy to see that, as x grows, the dipole cross section gets suppressed. (Keeping in mind the suppression by the photon wave function in the large- r region.) Such effect was discussed previously in Ref. [58] in the context of the BK equation. In fact, this suppression is the motivation given in Ref. [27] for such modification of x , so that, in the small- Q^2 limit, the total cross section remains finite. Since

$$\left(1 + \frac{4m_f^2}{Q^2}\right) \leq \left(1 + \frac{k_T^2}{Q^2} + \frac{\kappa_T'^2 + m_f^2}{\beta(1-\beta)Q^2}\right), \tag{15}$$

the k_T -factorization case receives more suppression. Consequently, the normalization factor σ_0 rises to compensate the suppression. Therefore, one can understand the change in σ_0 as a direct consequence of the key difference between the k_T -factorization and the dipole factorization.

4 Dijet production at EIC

The F_2 structure function is an inclusive object and it is weakly sensitive to the shape of the gluon density. To probe that shape better, we shall now apply the dipole cross sections obtained in the previous section to the jet correlations at the EIC, following closely the method of Ref. [41].

We consider dijet production in DIS

$$e + p \rightarrow e + J_1 + J_2 + X. \tag{16}$$

At the leading order, in the small- x limit, this process is dominated by $q\bar{q}$ jets [12]. It is therefore closely related to the dipole picture we discussed earlier. In the Breit frame, where the photon momentum is given by $q = (0, 0, 0, Q)$, at the leading order, the jets momentum imbalance $p_T \equiv |p_{1T} + p_{2T}|$ equals the gluon transverse momentum k_T , where p_{1T} and p_{2T} are transverse momenta of the jets. This makes dijets an interesting process. For the region where $p_T \ll P_T \sim p_{1T}, p_{2T}$, one may use power counting to take leading order in p_T/P_T , which leads to the transverse-momentum-dependent (TMD) factorization.

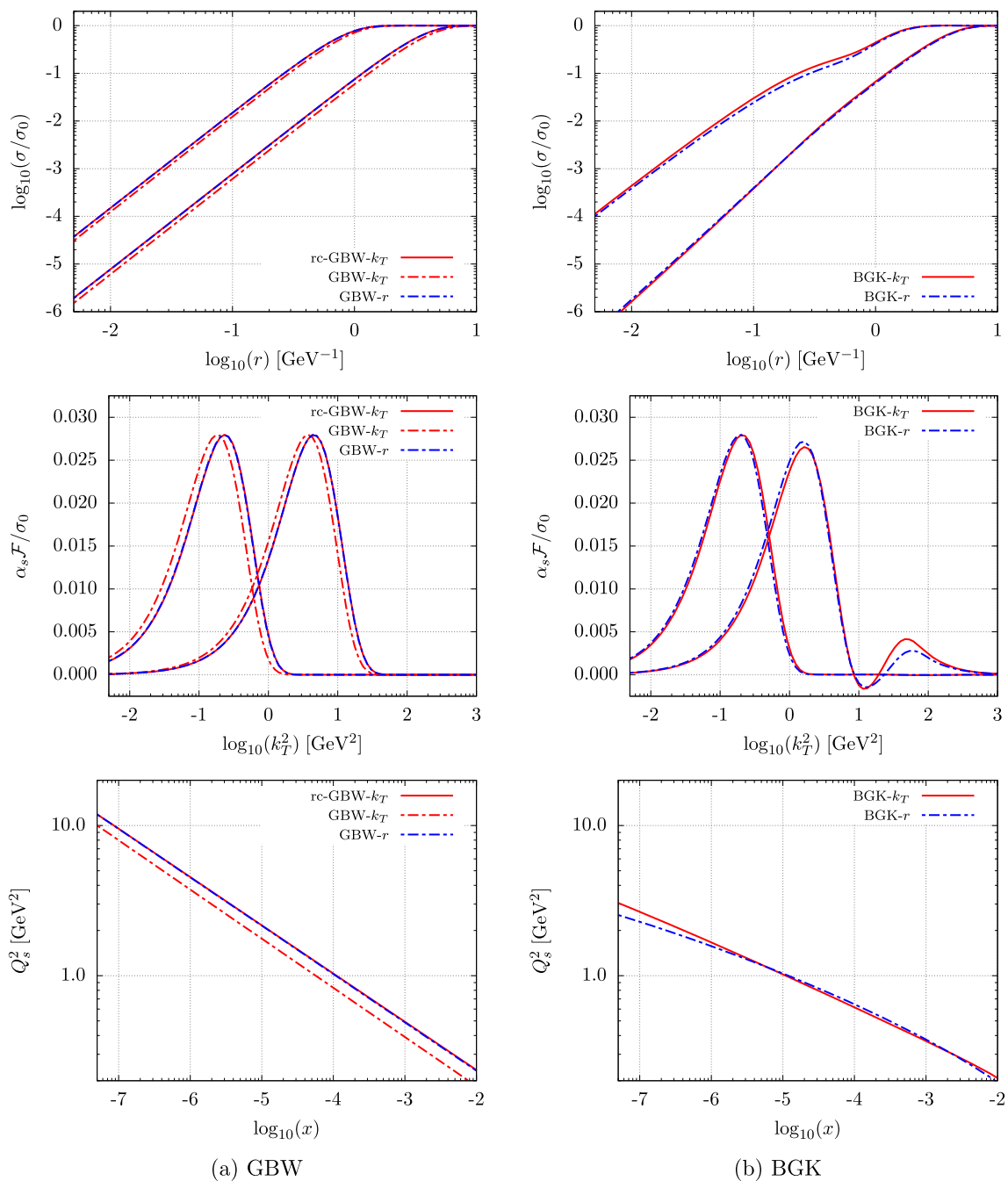


Fig. 2 The dipole cross section, the dipole gluon density at $x = 10^{-2}, 10^{-6}$, and the saturation scale for the GBW (left) and the BGK (right) models. Note that the dipole cross section and the gluon density are normalized with σ_0^{-1}

In the large- N_c limit of the TMD factorization, there are two types of gluon densities, namely the dipole gluon density and the Weizsäcker–Williams (WW) gluon density [11, 12, 60, 61]. It was shown in Ref. [12], that the dijet process in DIS can directly probe the WW gluon, $\mathcal{F}^{\text{WW}}(x, k^2)$, where the differential cross section factorizes as

$$\frac{d\sigma^{\gamma^* p \rightarrow q\bar{q}X}}{d\text{P.S.}} = \mathcal{F}^{\text{WW}}(x, k_T^2) H_{\gamma^* g^* \rightarrow q\bar{q}}, \quad (17)$$

with the hard function $H_{\gamma^* g^* \rightarrow q\bar{q}}$ describing interactions of an off-shell photon with an off-shell gluon producing a $q\bar{q}$ pair. $\mathcal{F}^{\text{WW}}(x, k^2)$, has an interpretation as a number density of gluons inside a proton, while $\mathcal{F}^{\text{dipole}}(x, k_T^2)$ does not have such an interpretation [11, 12, 61].

We carry out our study in the framework of the *Improved Transverse-Momentum-Dependent* (ITMD) factorization [60,

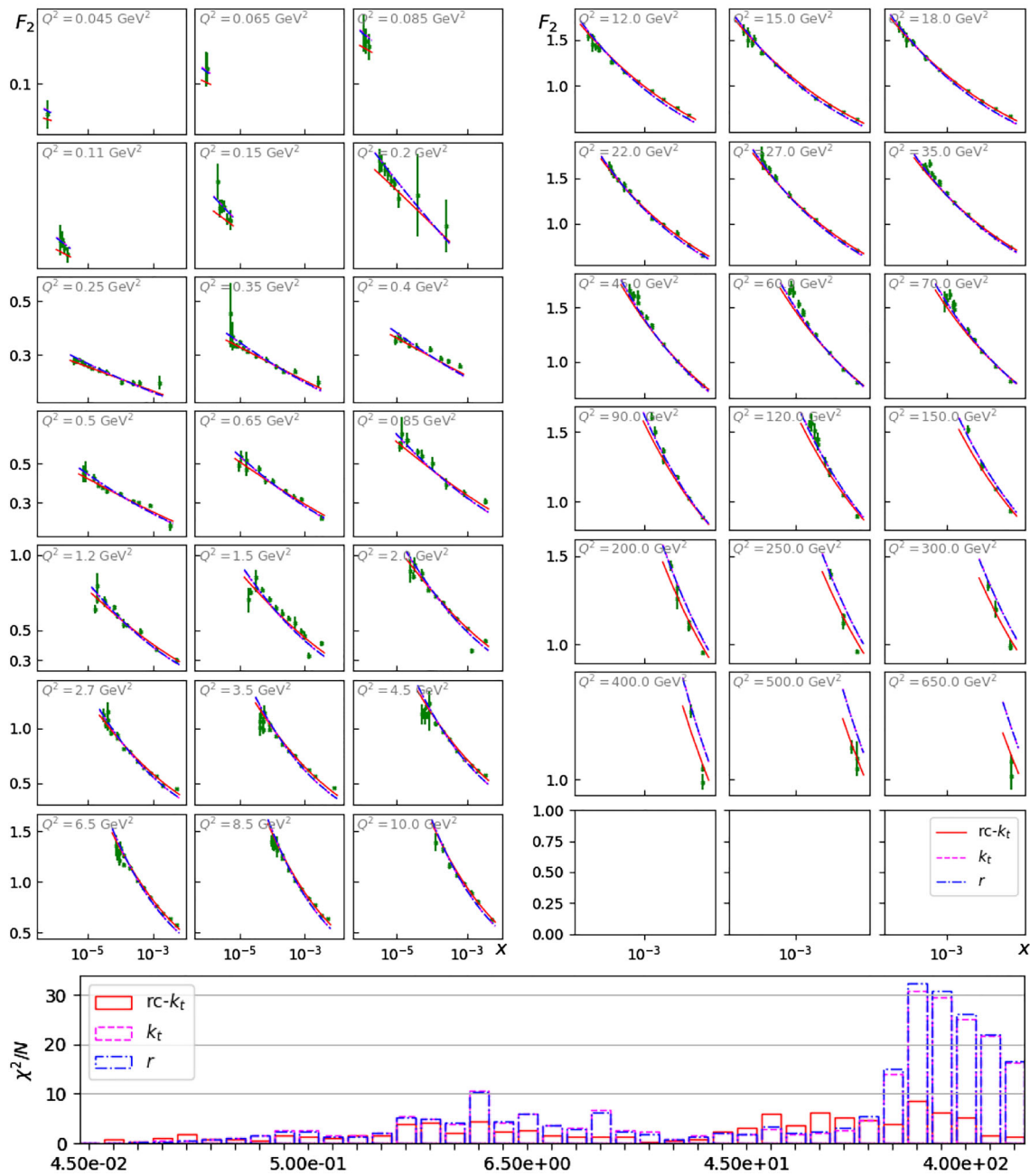


Fig. 3 Comparison of F_2 from GBW with HERA data. The histogram shows the χ^2 value per data point in each frame. Improvement by the running coupling (rc- k_T) is clearly visible in the high- Q^2 region, while the new fit (k_T) shows only marginal improvement

[62].³ This is implemented in the program KaTie [63], which we use to compute the cross sections. The ITMD factorization is a generalization of the TMD factorization, where the momentum imbalance in TMD is restricted to be small [60,62]. That is to say, ITMD resums $(Q_s/k_T)^n$ and $(k_T/P_T)^n$ [60,62], thus extends the region of applicability up to $k_T \sim P_T$. The difference of Eq. (17) from the regu-

lar TMD is that the hard function has an off-shell gluon, g^* , thus rendering the k_T dependence in the hard function as well [62].

Under the Gaussian approximation and assuming θ -like profile of the proton, one can write [11, 12, 60, 61]

$$\mathcal{F}^{\text{WW}}(x, k^2) = \frac{C_F}{2\pi^3\alpha_s} \int_0^\infty \frac{dr}{r} J_0(rk) \sigma_{\text{dipole Adj.}}(x, r), \quad (18)$$

³ We limit ourselves to unpolarized contribution as it is the leading one. For the polarized one, see Ref. [38].

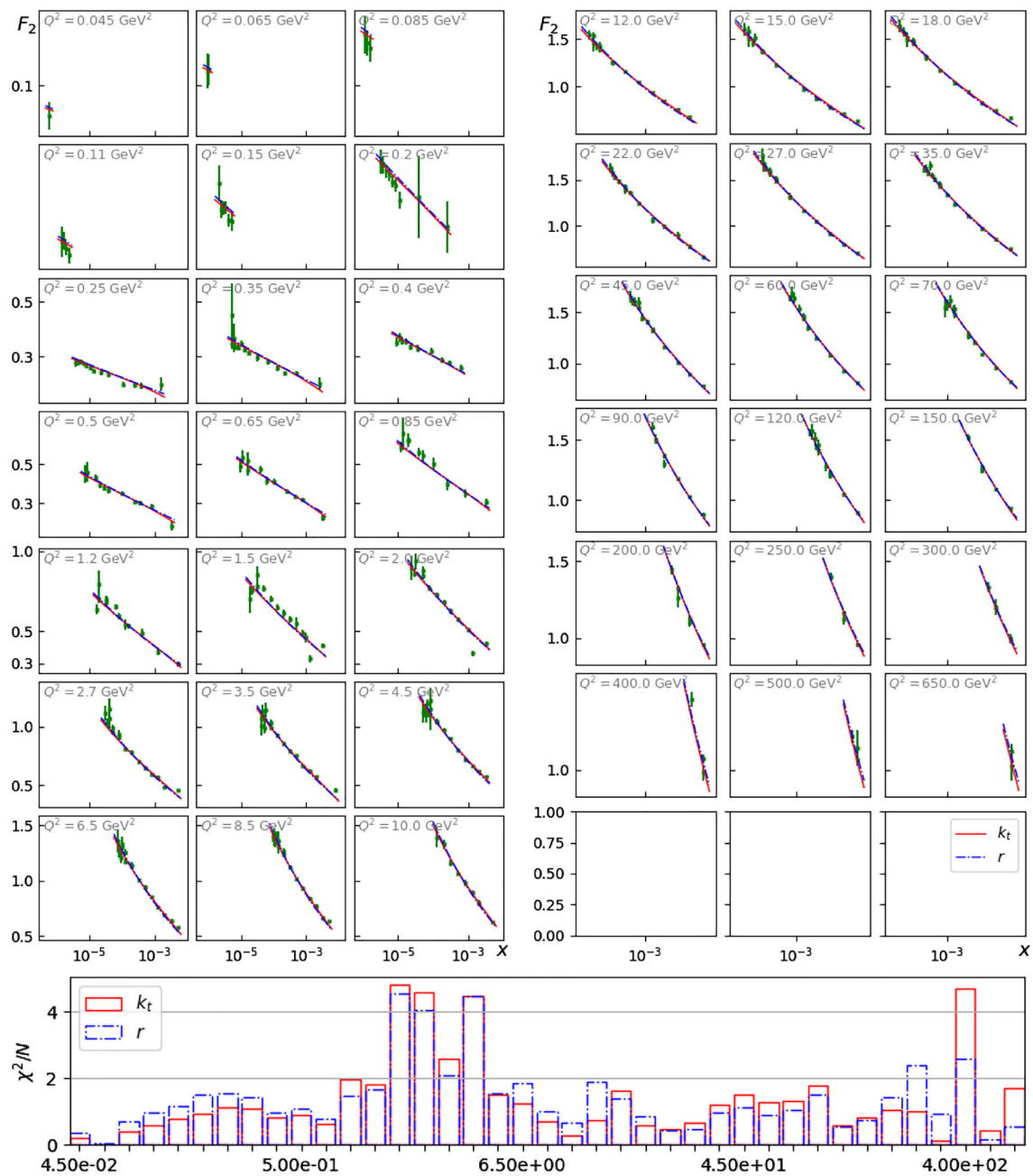


Fig. 4 Comparison of F_2 from BGK with HERA data. The histogram shows the χ^2 value per data point in each frame. The overall fit quality remain similar but the quality in each frame changes noticeably. In particularly, the k_T -formula (k_T) shows better quality at small Q^2

with the adjoint dipole cross section

$$\sigma_{\text{dipole Adj.}}(x, r) = \sigma_0 \left(1 - \left(1 - \frac{\sigma_{\text{dipole}}(x, r)}{\sigma_0} \right)^{C_A/C_F} \right). \tag{19}$$

For the region where the TMD factorization is applicable, $Q_s \sim k_T \ll P_T \sim Q$, one needs to resum the large Sudakov logarithms $\log(k_T/Q)$, as well as $\log(1/x)$ [12]. It was shown in Refs. [13, 64, 65] that consistent resummation

of such logarithms is possible owing to the separation of corresponding regions (see also Ref. [66]). Resummation of the Sudakov logarithms is achieved by the formula

$$\begin{aligned} \mathcal{F}^{\text{WW}}(x, k^2, \mu^2) &= \frac{C_F}{2\pi^3 \alpha_s} \int_0^\infty \frac{dr}{r} J_0(rk) e^{-S(r, \mu^2)} \sigma_{\text{dipole Adj.}}(x, r), \tag{20} \end{aligned}$$

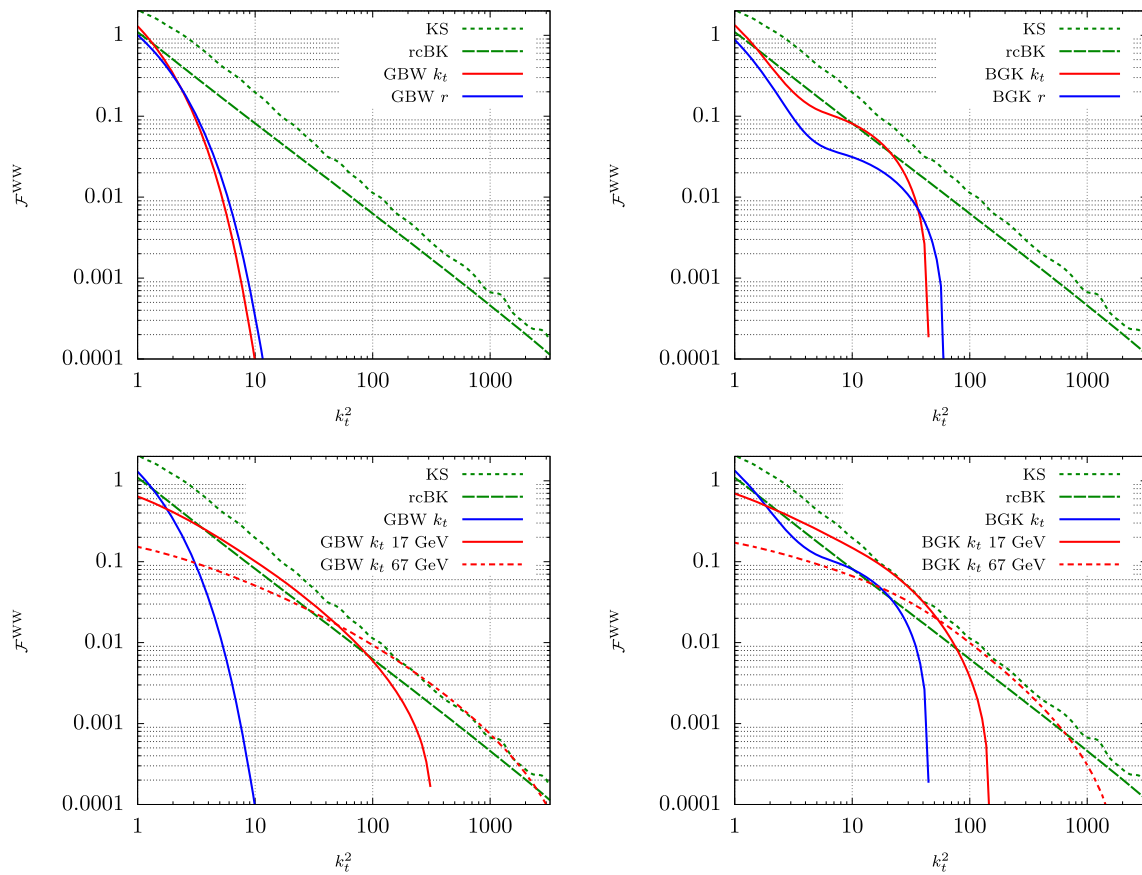


Fig. 5 Weizsäcker–Williams gluon density at $x = 10^{-3}$. Top row: Comparison of the dipole factorization fit and k_T -factorization fit results. Bottom row: Comparison of the respective models with and

without the Sudakov factor, at $\mu = 17, 67$ GeV. The green dotted line is the KS gluon [41], and the green dashed line is the rcBK gluon [59]

where, we use the Sudakov form factor [13, 65],

$$S(r, \mu^2) = \frac{\alpha_s N_c}{4\pi} \ln^2 \left(\frac{\mu^2 r^2}{4e^{-2\gamma_E}} \right), \tag{21}$$

in which γ_E is the Euler-Mascheroni constant, and we set $\alpha_s = 0.2$. The obtained gluon densities are shown in Fig. 5.

4.1 Comparison to HERA data

Before discussing dijet production at the EIC, we compare our model with inclusive dijet data from HERA [67]. The kinematical cuts chosen for this study read

$$\begin{aligned} E_p &= 27.6 \text{ GeV}, & E_e &= 920 \text{ GeV}, \\ p_{2T} &> 4 \text{ GeV}, & 5.0 &< \langle p_T \rangle_2 < 50 \text{ GeV}, \\ 0.2 &< y < 0.6, & -1.0 &< \eta_{1\text{Lab}}^{\text{jet}}, \eta_{2\text{Lab}}^{\text{jet}} < 2.5, \\ 5.5 &< Q^2 < 80 \text{ GeV}^2, \\ R &= \sqrt{(\Delta\eta_{\text{Lab}}^{\text{jet}})^2 + (\Delta\phi_{\text{Lab}}^{\text{jet}})^2} < 1, \end{aligned} \tag{22}$$

where the average transverse momentum of jets in the Breit frame is given by

$$\langle p_T \rangle_2 \equiv \frac{1}{2} (p_{1T} + p_{2T}), \tag{23}$$

and η and ϕ denote pseudo-rapidity and azimuthal angle, respectively. The processes under consideration are of the type

$$g \rightarrow q\bar{q}, \tag{24}$$

where we take five massless quark flavours [67].

The renormalization and factorization scales are given by⁴

$$\mu = \frac{1}{2} (Q + \langle p_T \rangle_2). \tag{25}$$

The comparison of the new and the old fits of the GBW and BGK models is shown in Fig. 6, in which we plot differential dijet cross sections in bins of $\langle p_T \rangle_2$ and Q^2 . In both cases of the GBW and BGK models, we observe that in the low- and moderate- Q^2 region, the new fits agree better with

⁴ Cf. Ref. [67], $\mu^2 = \frac{1}{2} (Q^2 + \langle p_T \rangle_2^2)$.

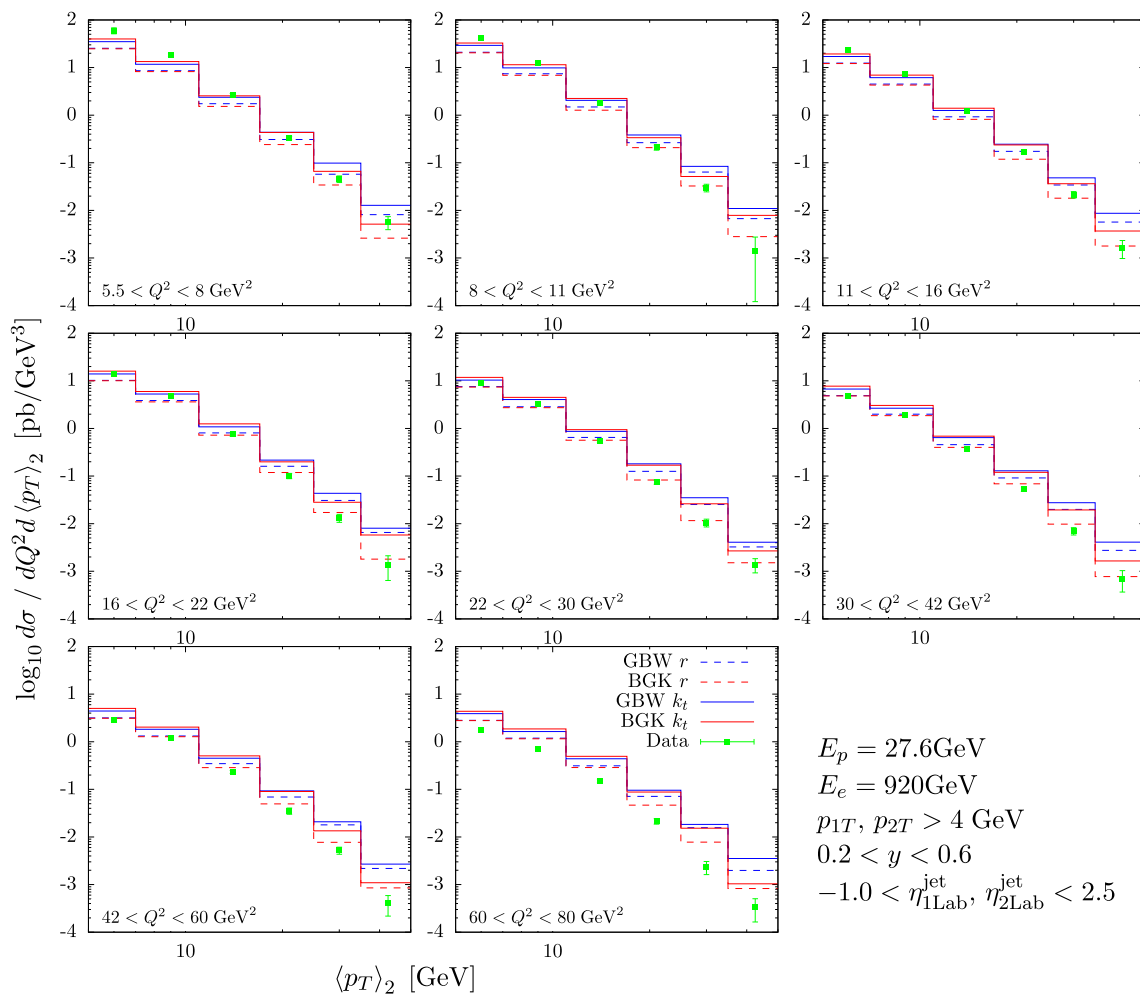


Fig. 6 Comparison of calculation with the GBW and BGK models, fitted in the dipole (r) and k_T factorization formulae to the HERA dijet data [67]

the data, except for large $\langle p_T \rangle_2$. At large Q^2 and large jet-transverse momenta, our predictions overshoot the data but this is expected, as this kinematic configurations lay beyond the validity region of the saturation models.

Figure 7 shows the effects of the Sudakov form factor in the case of the BGK model. Here, we plot the BGK model predictions with an uncertainty estimated by varying the renormalization scale by the factors 0.5 and 2. We see that the Sudakov form factor has a sizeable effect by making the $\langle p_T \rangle_2$ -spectra steeper. This leads to lowering the high- $\langle p_T \rangle_2$ region, which improves agreement with the data. Hence, we can conclude that the BGK model with exact kinematics and Sudakov resummation provides a good description of dijet production at HERA energies.

4.2 Dijet processes at EIC

Following Ref. [41], we study the azimuthal correlations of jets and the final state electron in DIS, where it was argued

that this observable is sensitive to the soft emissions and the saturation effects. In this study we focus only on the proton case. The kinematical cuts suggested in Ref. [41] are

$$E_e = 15\text{GeV}, \quad E_p = 135\text{GeV}, \quad Q^2 > 1\text{GeV}^2, \\ 0.1 < \nu < 0.85, \quad \Delta R_{\text{Breit}} < 1, \quad p_{1,2T}^{\text{Breit}} > 3\text{GeV}, \\ -4 < y_{1,2\text{lab}} < -1.$$

Grids of the Weizsäcker–Williams gluon density were produced by evaluating Eqs. (18) and (20). The gluon density at $x = 10^{-3}$ is plotted in Fig. 5 with the hard-scale-independent Kutak–Sapeta (KS) gluon [41,68,69] and the running-coupling BK (rcBK) gluon density [57,59,70]. Both of these gluon densities are solutions of evolution equations and treat better perturbative tail at large k_T . Furthermore, the KS gluon takes into account resummed corrections of higher orders, i.e. kinematical constraint and nonsingular (at low z) elements of DGLAP splitting functions [45].

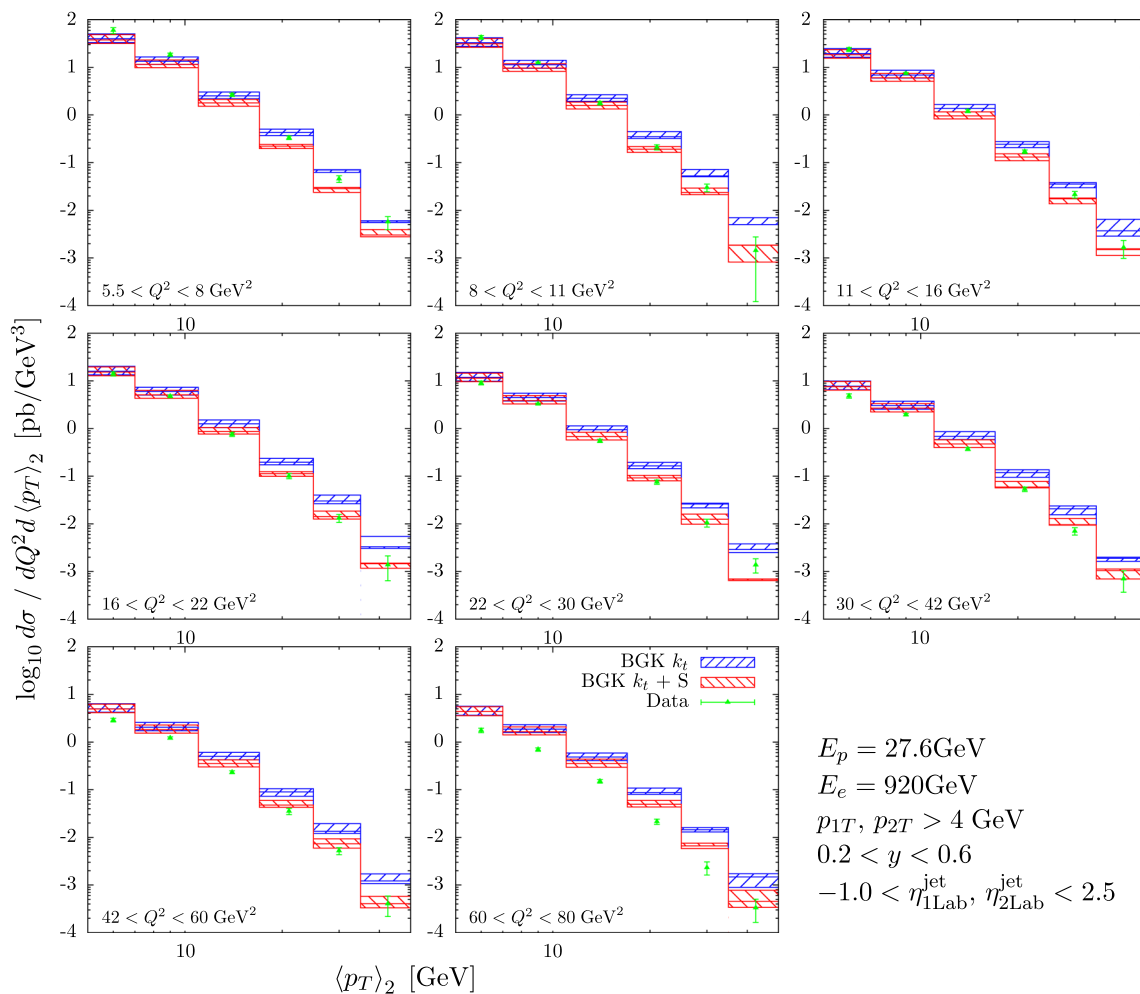


Fig. 7 Effects of Sudakov factor in the BGK model, fitted in the k_T factorization formula to the HERA dijet data [67]. Uncertainty was estimated by varying renormalization scale by multiplying by 0.5 and 2

Clearly, as shown in Fig. 5, the GBW and BGK models fall much more quickly than the KS and rcBK gluon densities. In general, expected behaviour in the large- k_T region is $\sim k_T^{-2}$ [11, 12], while σ_{GBW} behaves like $\sim e^{-k_T^2}$. As in Ref. [41], the Sudakov factor enhances in the small- k_T region and suppresses in the large- k_T region. In other words, it broadens the distribution. In comparison to the result of Ref. [41], the effect of broadening by the Sudakov factor is significantly more pronounced in the case of the GBW and BGK models. The hard-scale-dependent GBW and BGK models, as a consequence, become closer to the KS and rcBK gluons, cf. Fig. 2 of Ref. [41].

Figures 8 and 9 show electron-jets azimuthal correlation in the Breit and in the Lab frame, respectively. In the top row of Fig. 8, we see, for both the GBW and BGK models, better agreements of results with the KS and rcBK for the new k_T -factorization fits. However the overall normalization of the gluon density depends on the coupling α_s , which we assumed to be 0.2. Nevertheless, it shows clearly the effect of

the parameter σ_0 . In the middle and the bottom row, it shows the effects of the Sudakov form factor, which qualitatively agrees with that of Ref. [41], by lowering the cross section.

Figure 9 shows the electron-jets correlation in the Lab frame. Here, the difference between KS and GBW and BGK is more prominent, while rcBK shows similar pattern to the GBW and BGK models and therefore we can attribute the effects to importance of higher order corrections, as are accounted for in KS gluon. The effects of the Sudakov factor are similar to those in Ref. [41] at relatively high $\Delta\phi$, while at smaller $\Delta\phi$, the effect is reversed (i.e. the cross sections were slightly lowered in Ref. [41], while here, they are significantly increased).

Finally, Fig. 10 shows the jet-jet correlations in the Breit frame. Again, the GBW and BGK models exhibit considerable deviation from the KS gluon. The difference from the previous plot is the disagreement of the GBW/BGK models and the rcBK in the small- $\Delta\phi$ region. Similarly to the previous plots, the Sudakov factor affects the models some-

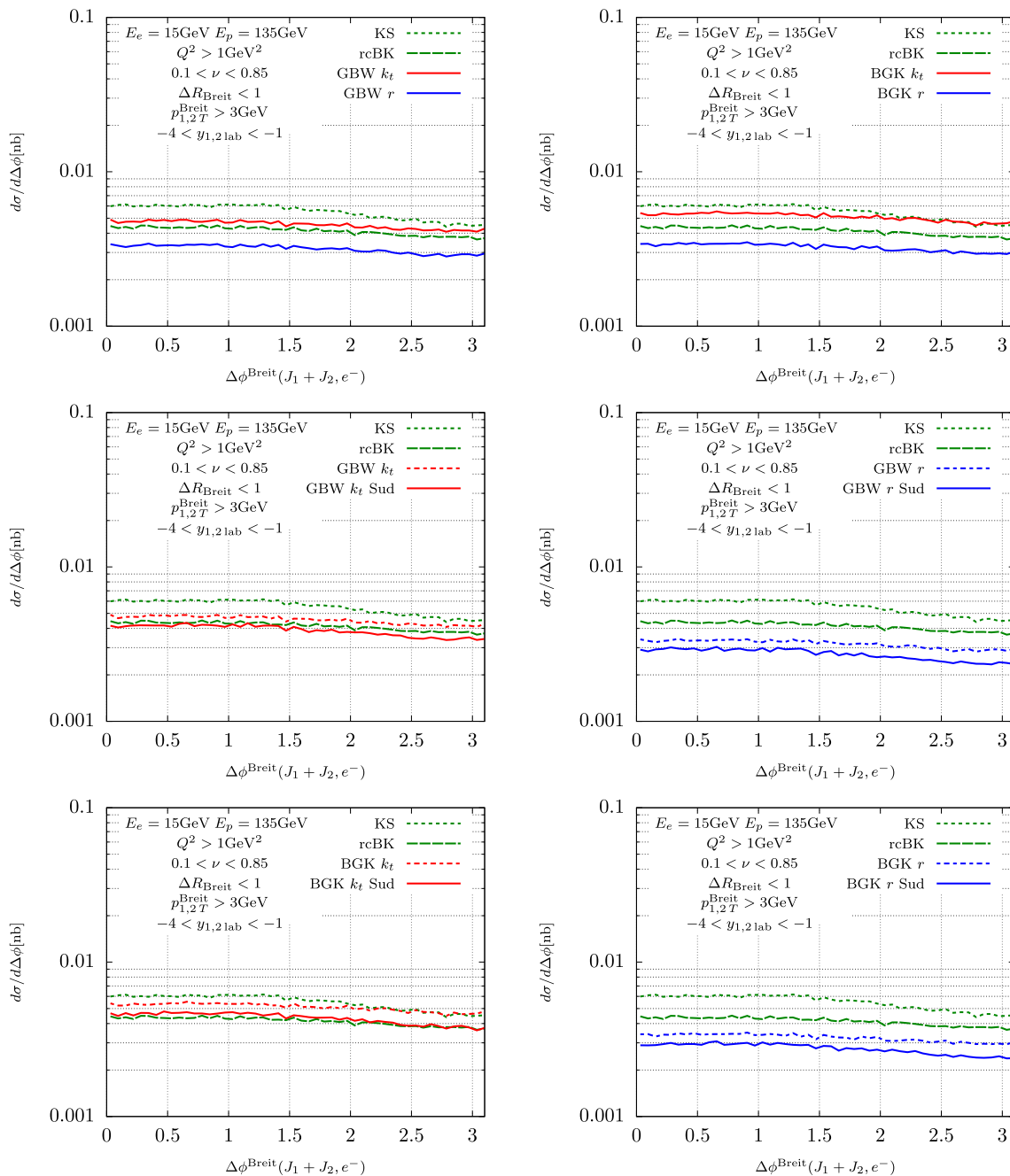


Fig. 8 Azimuthal correlation of the jets and the scattered electron in the Breit frame. Top: Comparison of dipole factorization fit and k_T -factorization fit. Middle and bottom: Effect of the Sudakov form factor.

what differently from the KS gluon in Ref. [41]. The effect enhances the cross section considerably in the small- $\Delta\phi$ region, making it closer to KS gluon result.

The results shown in Figs. 9 and 10 are natural, as back-to-back configuration in the respective observable corresponds to the small- k_T region of gluon densities and, as it can be seen clearly in Fig. 5, the GBW and BGK gluons do not fare well in the large- k_T region. That is to say that the enhancement in the

The green dotted line is the KS gluon [41], and the green dashed line is the rcBK gluon [59]

small- $\Delta\phi$ region is a direct consequence of the broadening by the Sudakov factor.

5 Summary

We have fitted the GBW and BGK saturation models to HERA data [33] using the k_T -factorization for the structure

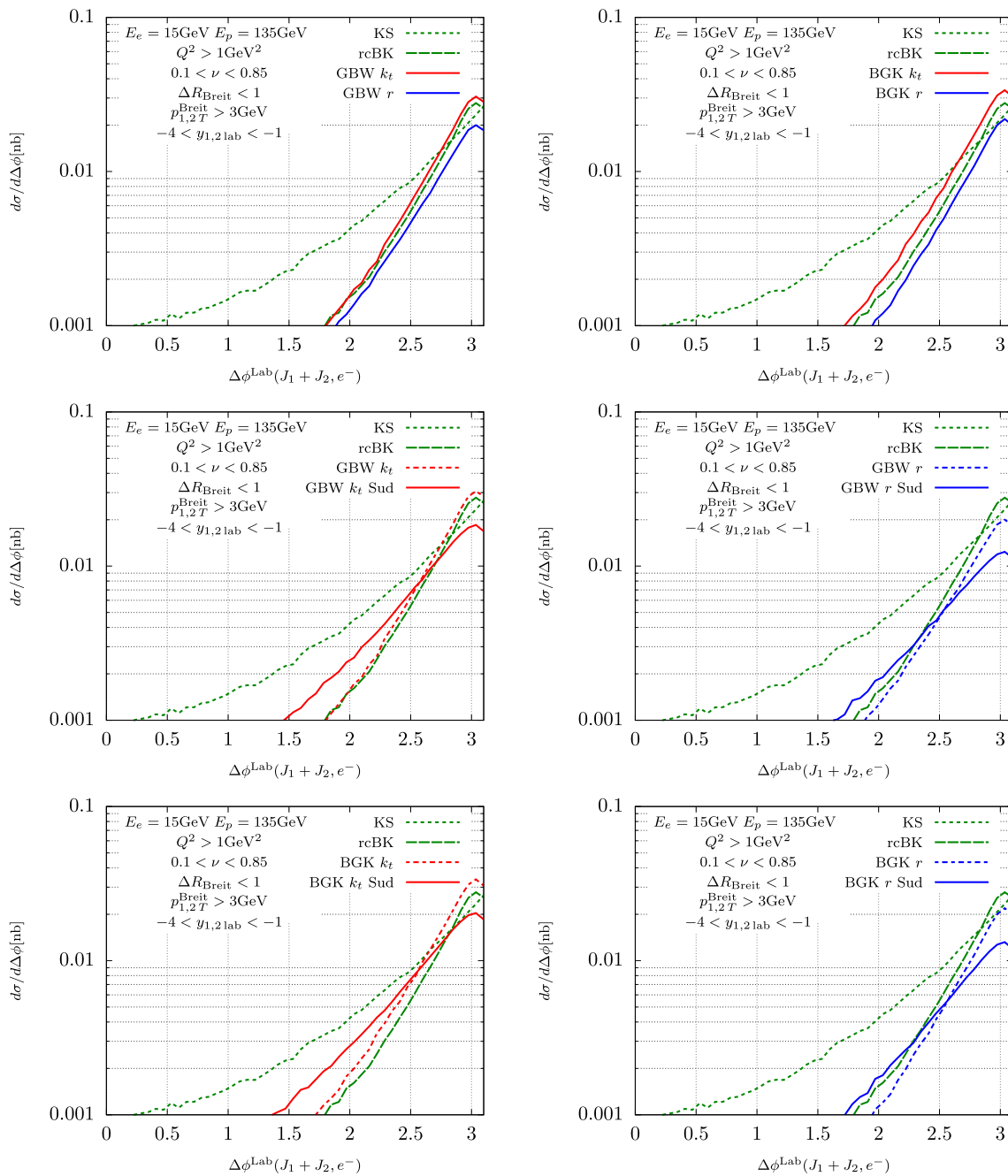


Fig. 9 Azimuthal correlation of the jets and the scattered electron in the lab frame. Top: Comparison of dipole factorization fit and k_T -factorization fit. Middle and bottom: Effect of the Sudakov form factor.

The green dotted line is the KS gluon [41], and the green dashed line is the rcBK gluon [59]

function F_2 . The main difference between the k_T - and the dipole factorizations is an argument of the gluon, x/z , appearing in the former and being replaced by $x(1 + 4m_f^2/Q^2)$ in the latter. In fact, the massive light quarks used in Ref. [27] partially simulate the factor $1/z$, and our fit result indicates such effect, as expected.

We found that the dipole factorization can reproduce the result of the k_T -factorization formula quite well. The

only major difference is in the normalization parameter σ_0 , which increases significantly for the k_T -factorization case. We argued that this change is a direct consequence of the kinematic approximation used in the dipole factorization formula. We have also observed that the explicit inclusion of the running coupling in the GBW model has a significant effect on fit quality, particularly in the large- Q^2 region, where the GBW model performs poorly.

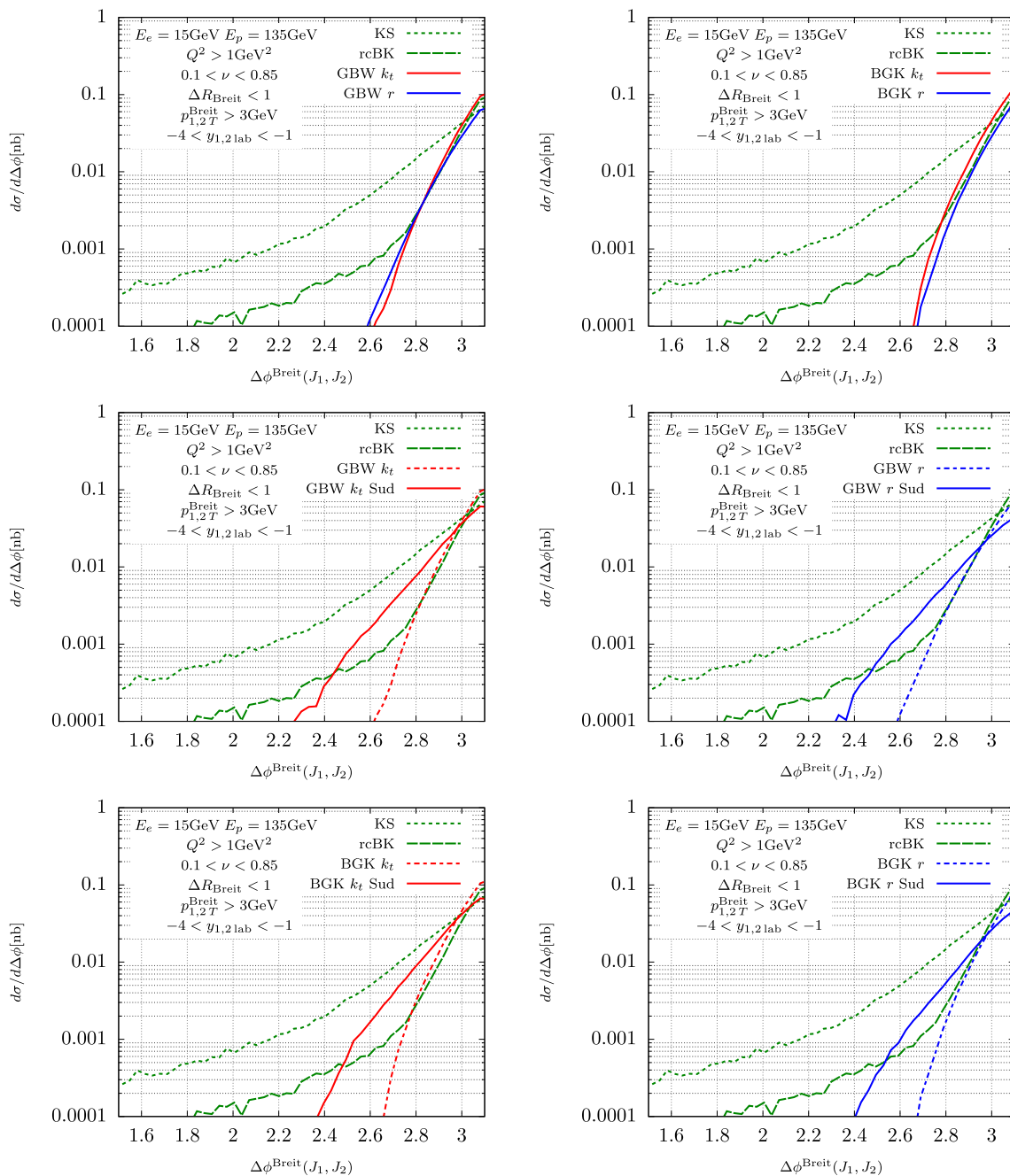


Fig. 10 Azimuthal correlation of the jets in the Breit frame. Top: Comparison of dipole factorization fit and k_T -factorization fit. Middle and bottom: Effect of the Sudakov form factor. The green dotted line is the KS gluon [41], and the green dashed line is the rcBK gluon [59]

We have applied the new results from our fits to description of the transverse momentum spectra of the dijet processes in DIS at HERA. The description of the data is fairly good with all used models. However, the best results are obtained within the k_T -BGK model with the Sudakov form factor, indicating the relevance of exact kinematics, DGLAP corrections, and resummation.

Furthermore, we provided predictions for dijet production at the EIC. Results of the electron-jets correlation in the Breit frame agrees qualitatively with those of Ref. [41]. Other results, namely the electron-jets in the Lab frame and the jet-jet correlation in the Breit frame, shows considerable effects of the Sudakov form factor, which broadens the gluon density.

Acknowledgements We are grateful to Krzysztof Golec-Biernat, Piotr Kotko and Andreas van Hameren for useful discussions. The project is partially supported by the European Union's Horizon 2020 research and innovation program under Grant agreement no. 824093. TG and SS are partially supported by the Polish National Science Centre Grant no. 2017/27/B/ST2/02004.

Data Availability Statement This manuscript has no associated data or the data will not be deposited. [Authors' comment: This is a theory paper and has no associated data or the data will not be deposited.]

Open Access This article is licensed under a Creative Commons Attribution 4.0 International License, which permits use, sharing, adaptation, distribution and reproduction in any medium or format, as long as you give appropriate credit to the original author(s) and the source, provide a link to the Creative Commons licence, and indicate if changes were made. The images or other third party material in this article are included in the article's Creative Commons licence, unless indicated otherwise in a credit line to the material. If material is not included in the article's Creative Commons licence and your intended use is not permitted by statutory regulation or exceeds the permitted use, you will need to obtain permission directly from the copyright holder. To view a copy of this licence, visit <http://creativecommons.org/licenses/by/4.0/>.

Funded by SCOAP³. SCOAP³ supports the goals of the International Year of Basic Sciences for Sustainable Development.

Appendix: I_i in Eq. (7)

The functions I_1 , I_2 , I_3 , I_4 used in Eq. (7) are defined as [44]

$$\begin{aligned} \frac{I_1}{2\pi} &= \frac{N_1 N_2 + N_3^2}{(N_1^2 + 2N_1 N_2 + N_3^2)^{3/2}}, \\ \frac{I_2}{2\pi} &= \frac{N_3 - (1 - \beta)N_1}{(N_1 + N_4)\sqrt{N_1^2 + 2N_1 N_2 + N_3^2}}, \\ \frac{I_3}{2\pi} &= \frac{N_1 + N_2}{(N_1^2 + 2N_1 N_2 + N_3^2)^{3/2}}, \\ \frac{I_4}{2\pi} &= \frac{2(1 - \beta)}{(N_1 + N_4)\sqrt{N_1^2 + 2N_1 N_2 + N_3^2}}, \end{aligned} \quad (26)$$

for

$$\begin{aligned} N_1 &\equiv \beta(1 - \beta)Q^2 + m_f^2, \\ N_2 &\equiv \kappa_T'^2 + (1 - \beta)^2 k_T^2, \\ N_3 &\equiv \kappa_T'^2 - (1 - \beta)^2 k_T^2, \\ N_4 &\equiv \kappa_T'^2 + \beta(1 - \beta)k_T^2. \end{aligned} \quad (27)$$

References

- R.G. Roberts, The Structure of the Proton (Cambridge University Press, Cambridge, 1994). ISBN 978-0-521-44944-1, 978-1-139-24244-8. <https://doi.org/10.1017/CBO9780511564062>
- J. Collins, *Cambridge Monographs on Particle Physics, Nuclear Physics and Cosmology*, vol. 32 (Cambridge University Press, Cambridge, 2011), pp. 1–624 (2011). ISBN 978-1-00-940184-5. <https://doi.org/10.1017/9781009401845>
- National Academies of Sciences, Engineering, and Medicine (The National Academies Press, 2018). ISBN:978-0-309-47856-4. <https://doi.org/10.17226/25171>
- S. Catani, M. Ciafaloni, F. Hautmann, Phys. Lett. B **242**, 97–102 (1990). [https://doi.org/10.1016/0370-2693\(90\)91601-7](https://doi.org/10.1016/0370-2693(90)91601-7)
- S. Catani, M. Ciafaloni, F. Hautmann, Nucl. Phys. B **366**, 135–188 (1991). [https://doi.org/10.1016/0550-3213\(91\)90055-3](https://doi.org/10.1016/0550-3213(91)90055-3)
- J.C. Collins, R.K. Ellis, Nucl. Phys. B **360**, 3–30 (1991). [https://doi.org/10.1016/0550-3213\(91\)90288-9](https://doi.org/10.1016/0550-3213(91)90288-9)
- S. Catani, M. Ciafaloni, F. Hautmann, Phys. Lett. B **307**, 147–153 (1993). [https://doi.org/10.1016/0370-2693\(93\)90204-U](https://doi.org/10.1016/0370-2693(93)90204-U)
- S. Catani, F. Hautmann, Phys. Lett. B **315**, 157–163 (1993). [https://doi.org/10.1016/0370-2693\(93\)90174-G](https://doi.org/10.1016/0370-2693(93)90174-G)
- S. Catani, F. Hautmann, Nucl. Phys. B **427**, 475–524 (1994). [https://doi.org/10.1016/0550-3213\(94\)90636-X](https://doi.org/10.1016/0550-3213(94)90636-X). arXiv:hep-ph/9405388
- C.J. Bomhof, P.J. Mulders, F. Pijlman, Eur. Phys. J. C **47**, 147–162 (2006). <https://doi.org/10.1140/epjc/s2006-02554-2>. arXiv:hep-ph/0601171
- F. Dominguez, B.W. Xiao, F. Yuan, Phys. Rev. Lett. **106**, 022301 (2011). <https://doi.org/10.1103/PhysRevLett.106.022301>. arXiv:1009.2141 [hep-ph]
- F. Dominguez, C. Marquet, B.W. Xiao, F. Yuan, Phys. Rev. D **83**, 105005 (2011). <https://doi.org/10.1103/PhysRevD.83.105005>. arXiv:1101.0715 [hep-ph]
- B.W. Xiao, F. Yuan, J. Zhou, Nucl. Phys. B **921**, 104–126 (2017). <https://doi.org/10.1016/j.nuclphysb.2017.05.012>. arXiv:1703.06163 [hep-ph]
- I.I. Balitsky, L.N. Lipatov, Sov. J. Nucl. Phys. **28**, 822–829 (1978)
- E.A. Kuraev, L.N. Lipatov, V.S. Fadin, Sov. Phys. JETP **45**, 199–204 (1977)
- Y.V. Kovchegov, E. Levin, *Cambridge Monographs on Particle Physics, Nuclear Physics and Cosmology*, vol. 33 (Oxford University Press, Oxford, 2012), pp. 1–350 (2012). <https://doi.org/10.1017/9781009291446>. ISBN:978-1-00-929144-6, 978-1-00-929141-5, 978-1-00-929142-2, 978-0-521-11257-4, 978-1-139-55768-9
- V. Barone, M. Genovese, N.N. Nikolaev, E. Predazzi, B.G. Zakharov, Phys. Lett. B **326**, 161–167 (1994). [https://doi.org/10.1016/0370-2693\(94\)91208-4](https://doi.org/10.1016/0370-2693(94)91208-4). arXiv:hep-ph/9307248
- L.V. Gribov, E.M. Levin, M.G. Ryskin, Phys. Rep. **100**, 1–150 (1983). [https://doi.org/10.1016/0370-1573\(83\)90022-4](https://doi.org/10.1016/0370-1573(83)90022-4)
- I. Balitsky, Nucl. Phys. B **463**, 99–160 (1996). [https://doi.org/10.1016/0550-3213\(95\)00638-9](https://doi.org/10.1016/0550-3213(95)00638-9). arXiv:hep-ph/9509348
- Y.V. Kovchegov, Phys. Rev. D **60**, 034008 (1999). <https://doi.org/10.1103/PhysRevD.60.034008>. arXiv:hep-ph/9901281
- A. Kovner, J.G. Milhano, Phys. Rev. D **61**, 014012 (2000). <https://doi.org/10.1103/PhysRevD.61.014012>. arXiv:hep-ph/9904420
- A. Kovner, J.G. Milhano, H. Weigert, Phys. Rev. D **62**, 114005 (2000). <https://doi.org/10.1103/PhysRevD.62.114005>. arXiv:hep-ph/0004014
- E. Iancu, A. Leonidov, L.D. McLerran, Nucl. Phys. A **692**, 583–645 (2001). [https://doi.org/10.1016/S0375-9474\(01\)00642-X](https://doi.org/10.1016/S0375-9474(01)00642-X). arXiv:hep-ph/0011241
- J. Jalilian-Marian, A. Kovner, H. Weigert, Phys. Rev. D **59**, 014015 (1998). <https://doi.org/10.1103/PhysRevD.59.014015>. arXiv:hep-ph/9709432
- J. Jalilian-Marian, A. Kovner, A. Leonidov, H. Weigert, Phys. Rev. D **59**, 014014 (1998). <https://doi.org/10.1103/PhysRevD.59.014014>. arXiv:hep-ph/9706377
- J. Jalilian-Marian, A. Kovner, A. Leonidov, H. Weigert, Nucl. Phys. B **504**, 415–431 (1997). [https://doi.org/10.1016/S0550-3213\(97\)00440-9](https://doi.org/10.1016/S0550-3213(97)00440-9). arXiv:hep-ph/9701284

27. K.J. Golec-Biernat, M. Wüsthoff, Phys. Rev. D **59**, 014017 (1998). <https://doi.org/10.1103/PhysRevD.59.014017>. [arXiv:hep-ph/9807513](https://arxiv.org/abs/hep-ph/9807513)
28. J. Bartels, K.J. Golec-Biernat, H. Kowalski, Phys. Rev. D **66**, 014001 (2002). <https://doi.org/10.1103/PhysRevD.66.014001>. [arXiv:hep-ph/0203258](https://arxiv.org/abs/hep-ph/0203258)
29. H. Kowalski, D. Teaney, Phys. Rev. D **68**, 114005 (2003). <https://doi.org/10.1103/PhysRevD.68.114005>. [arXiv:hep-ph/0304189](https://arxiv.org/abs/hep-ph/0304189)
30. L.D. McLerran, R. Venugopalan, Phys. Rev. D **49**, 2233–2241 (1994). <https://doi.org/10.1103/PhysRevD.49.2233>. [arXiv:hep-ph/9309289](https://arxiv.org/abs/hep-ph/9309289)
31. J.R. Forshaw, G. Kerley, G. Shaw, Phys. Rev. D **60**, 074012 (1999). <https://doi.org/10.1103/PhysRevD.60.074012>. [arXiv:hep-ph/9903341](https://arxiv.org/abs/hep-ph/9903341)
32. E. Iancu, K. Itakura, S. Munier, Phys. Lett. B **590**, 199–208 (2004). <https://doi.org/10.1016/j.physletb.2004.02.040>. [arXiv:hep-ph/0310338](https://arxiv.org/abs/hep-ph/0310338)
33. I. Abt, A.M. Cooper-Sarkar, B. Foster, V. Myronenko, K. Wichmann, M. Wing, Phys. Rev. D **96**(1), 014001 (2017). <https://doi.org/10.1103/PhysRevD.96.014001>. [arXiv:1704.03187](https://arxiv.org/abs/1704.03187) [hep-ex]
34. A.H. Mueller, B. Patel, Nucl. Phys. B **425**, 471–488 (1994). [https://doi.org/10.1016/0550-3213\(94\)90284-4](https://doi.org/10.1016/0550-3213(94)90284-4). [arXiv:hep-ph/9403256](https://arxiv.org/abs/hep-ph/9403256)
35. R. Abdul Khalek, A. Accardi, J. Adam, D. Adamiak, W. Akers, M. Albaladejo, A. Al-bataineh, M.G. Alexeev, F. Ameli, P. Antonioli et al., Nucl. Phys. A **1026**, 122447 (2022). <https://doi.org/10.1016/j.nuclphysa.2022.122447>. [arXiv:2103.05419](https://arxiv.org/abs/2103.05419) [physics.ins-det]
36. P. Caucal, F. Salazar, B. Schenke, T. Stebel, R. Venugopalan, JHEP **08**, 062 (2023). [https://doi.org/10.1007/JHEP08\(2023\)062](https://doi.org/10.1007/JHEP08(2023)062). [arXiv:2304.03304](https://arxiv.org/abs/2304.03304) [hep-ph]
37. P. Caucal, F. Salazar, R. Venugopalan, JHEP **11**, 222 (2021). [https://doi.org/10.1007/JHEP11\(2021\)222](https://doi.org/10.1007/JHEP11(2021)222). [arXiv:2108.06347](https://arxiv.org/abs/2108.06347) [hep-ph]
38. R. Boussarie, H. Mäntysaari, F. Salazar, B. Schenke, JHEP **09**, 178 (2021). [https://doi.org/10.1007/JHEP09\(2021\)178](https://doi.org/10.1007/JHEP09(2021)178). [arXiv:2106.11301](https://arxiv.org/abs/2106.11301) [hep-ph]
39. P. Taels, T. Altinoluk, G. Beuf, C. Marquet, JHEP **10**, 184 (2022). [https://doi.org/10.1007/JHEP10\(2022\)184](https://doi.org/10.1007/JHEP10(2022)184). [arXiv:2204.11650](https://arxiv.org/abs/2204.11650) [hep-ph]
40. T. Altinoluk, R. Boussarie, C. Marquet, P. Taels, JHEP **07**, 079 (2019). [https://doi.org/10.1007/JHEP07\(2019\)079](https://doi.org/10.1007/JHEP07(2019)079). [arXiv:1810.11273](https://arxiv.org/abs/1810.11273) [hep-ph]
41. A. van Hameren, P. Kotko, K. Kutak, S. Sapeta, E. Żarów, Eur. Phys. J. C **81**, 741 (2021). <https://doi.org/10.1140/epjc/s10052-021-09529-3>. [arXiv:2106.13964](https://arxiv.org/abs/2106.13964) [hep-ph]
42. K.J. Golec-Biernat, M. Wüsthoff, Phys. Rev. D **60**, 114023 (1999). <https://doi.org/10.1103/PhysRevD.60.114023>. [arXiv:hep-ph/9903358](https://arxiv.org/abs/hep-ph/9903358)
43. A. Bialas, H. Navelet, R.B. Peschanski, Nucl. Phys. B **593**, 438–450 (2001). [https://doi.org/10.1016/S0550-3213\(00\)00640-4](https://doi.org/10.1016/S0550-3213(00)00640-4). [arXiv:hep-ph/0009248](https://arxiv.org/abs/hep-ph/0009248)
44. M. Kimber, *Unintegrated parton distributions*. PhD thesis, Durham University
45. J. Kwiecinski, A.D. Martin, A.M. Stasto, Phys. Rev. D **56**, 3991–4006 (1997). <https://doi.org/10.1103/PhysRevD.56.3991>. [arXiv:hep-ph/9703445](https://arxiv.org/abs/hep-ph/9703445)
46. N.N. Nikolaev, B.G. Zakharov, Z. Phys. C **49**, 607–618 (1991). <https://doi.org/10.1007/BF01483577>
47. A. Łuszczak, M. Łuszczak, W. Schäfer, Phys. Lett. B **835**, 137582 (2022). <https://doi.org/10.1016/j.physletb.2022.137582>. [arXiv:2210.02877](https://arxiv.org/abs/2210.02877) [hep-ph]
48. G. Beuf, H. Hänninen, T. Lappi, H. Mäntysaari, Phys. Rev. D **102**, 074028 (2020). <https://doi.org/10.1103/PhysRevD.102.074028>. [arXiv:2007.01645](https://arxiv.org/abs/2007.01645) [hep-ph]
49. K.S. Kölbig, Comput. Phys. Commun. **4**(2), 221–226 (1972). [https://doi.org/10.1016/0010-4655\(72\)90012-4](https://doi.org/10.1016/0010-4655(72)90012-4). <https://www.sciencedirect.com/science/article/pii/0010465572900124>
50. M. Galassi, J. Davies, J. Theiler, B. Gough, G. Jungman, *GNU Scientific Library-Reference Manual*, Third Edition, for GSL Version 1.12, 3rd edn. (2009). ISBN:978-0-9546120-7-8
51. T. Hahn, Comput. Phys. Commun. **168**, 78–95 (2005). <https://doi.org/10.1016/j.cpc.2005.01.010>. [arXiv:hep-ph/0404043](https://arxiv.org/abs/hep-ph/0404043)
52. R. Brun, F. Rademakers, Nucl. Instrum. Methods A **389**, 81–86 (1997). [https://doi.org/10.1016/S0168-9002\(97\)00048-X](https://doi.org/10.1016/S0168-9002(97)00048-X)
53. F. James, M. Winkler, *MINUIT User's Guide* (2004)
54. T. Goda, K. Kutak, S. Sapeta, Nucl. Phys. B **990**, 116155 (2023). <https://doi.org/10.1016/j.nuclphysb.2023.116155>. [arXiv:2210.16084](https://arxiv.org/abs/2210.16084) [hep-ph]
55. J.L. Albacete, N. Armesto, J.G. Milhano, C.A. Salgado, U.A. Wiedemann, Phys. Rev. D **71**, 014003 (2005). <https://doi.org/10.1103/PhysRevD.71.014003>. [arXiv:hep-ph/0408216](https://arxiv.org/abs/hep-ph/0408216)
56. J.L. Albacete, Y.V. Kovchegov, Phys. Rev. D **75**, 125021 (2007). <https://doi.org/10.1103/PhysRevD.75.125021>. [arXiv:0704.0612](https://arxiv.org/abs/0704.0612) [hep-ph]
57. J.L. Albacete, N. Armesto, J.G. Milhano, P. Quiroga-Arias, C.A. Salgado, Eur. Phys. J. C **71**, 1705 (2011). <https://doi.org/10.1140/epjc/s10052-011-1705-3>. [arXiv:1012.4408](https://arxiv.org/abs/1012.4408) [hep-ph]
58. K. Kutak, A.M. Stasto, Eur. Phys. J. C **41**, 343–351 (2005). <https://doi.org/10.1140/epjc/s2005-02223-0>. [arXiv:hep-ph/0408117](https://arxiv.org/abs/hep-ph/0408117)
59. M. Hentschinski, K. Kutak, R. Straka, Eur. Phys. J. C **82**(12), 1147 (2022). <https://doi.org/10.1140/epjc/s10052-022-11122-1>. [arXiv:2207.09430](https://arxiv.org/abs/2207.09430) [hep-ph]
60. A. van Hameren, P. Kotko, K. Kutak, C. Marquet, E. Petreska, S. Sapeta, JHEP **12**, 034 (2016). [https://doi.org/10.1007/JHEP12\(2016\)034](https://doi.org/10.1007/JHEP12(2016)034). [arXiv:1607.03121](https://arxiv.org/abs/1607.03121) [hep-ph]. [Erratum: JHEP **02**, 158 (2019)]
61. B.W. Xiao, Nucl. Phys. A **967**, 257–264 (2017). <https://doi.org/10.1016/j.nuclphysa.2017.05.024>. [arXiv:1704.03662](https://arxiv.org/abs/1704.03662) [nucl-th]
62. P. Kotko, K. Kutak, C. Marquet, E. Petreska, S. Sapeta, A. van Hameren, JHEP **09**, 106 (2015). [https://doi.org/10.1007/JHEP09\(2015\)106](https://doi.org/10.1007/JHEP09(2015)106). [arXiv:1503.03421](https://arxiv.org/abs/1503.03421) [hep-ph]
63. A. van Hameren, Comput. Phys. Commun. **224**, 371–380 (2018). <https://doi.org/10.1016/j.cpc.2017.11.005>. [arXiv:1611.00680](https://arxiv.org/abs/1611.00680) [hep-ph]
64. A.H. Mueller, B.W. Xiao, F. Yuan, Phys. Rev. Lett. **110**(8), 082301 (2013). <https://doi.org/10.1103/PhysRevLett.110.082301>. [arXiv:1210.5792](https://arxiv.org/abs/1210.5792) [hep-ph]
65. A.H. Mueller, B.W. Xiao, F. Yuan, Phys. Rev. D **88**(11), 114010 (2013). <https://doi.org/10.1103/PhysRevD.88.114010>. [arXiv:1308.2993](https://arxiv.org/abs/1308.2993) [hep-ph]
66. M. Nefedov, Phys. Rev. D **104**(5), 054039 (2021). <https://doi.org/10.1103/PhysRevD.104.054039>. [arXiv:2105.13915](https://arxiv.org/abs/2105.13915) [hep-ph]
67. V. Andreev et al. (H1), Eur. Phys. J. C **77**(4), 215 (2017). <https://doi.org/10.1140/epjc/s10052-017-4717-9>. [arXiv:1611.03421](https://arxiv.org/abs/1611.03421) [hep-ex]. [Erratum: Eur. Phys. J. C **81**(8), 739 (2021)]
68. K. Kutak, S. Sapeta, Phys. Rev. D **86**, 094043 (2012). <https://doi.org/10.1103/PhysRevD.86.094043>. [arXiv:1205.5035](https://arxiv.org/abs/1205.5035) [hep-ph]
69. N.A. Abdulov, A. Bacchetta, S. Baranov, A. Bermudez Martinez, V. Bertone, C. Bissolotti, V. Candilise, L.I.E. Banos, M. Bury, P.L.S. Connor et al., Eur. Phys. J. C **81**, 752 (2021). <https://doi.org/10.1140/epjc/s10052-021-09508-8>. [arXiv:2103.09741](https://arxiv.org/abs/2103.09741) [hep-ph]
70. I. Balitsky, Phys. Rev. D **75**, 014001 (2007). <https://doi.org/10.1103/PhysRevD.75.014001>. [arXiv:hep-ph/0609105](https://arxiv.org/abs/hep-ph/0609105)